Identification of a Degradation Signal Sequence within Substrates of the Mitochondrial i-AAA Protease

Anthony J. Rampello and Steven E. Glynn

Department of Biochemistry and Cell Biology, *Stony Brook University, Stony Brook, NY, 11794-5215, USA*

Correspondence to Steven E. Glynn: *steven.glynn@stonybrook.edu.*
http://dx.doi.org/10.1016/j.jmb.2017.02.009
Edited by Yigong Shi

Abstract

The i-AAA protease is a component of the mitochondrial quality control machinery that regulates respiration, mitochondrial dynamics, and protein import. The protease is required to select specific substrates for degradation from among the diverse complement of proteins present in mitochondria, yet the rules that govern this selection are unclear. Here, we reconstruct the yeast i-AAA protease, Yme1p, to examine the *in vitro* degradation of two intermembrane space chaperone subunits, Tim9 and Tim10. Yme1p degrades Tim10 more rapidly than Tim9 despite high sequence and structural similarity, and loss of Tim10 is accelerated by the disruption of conserved disulfide bonds within the substrate. An unstructured N-terminal region of Tim10 is necessary and sufficient to target the substrate to the protease through recognition of a short phenylalanine-rich motif, and the presence of similar motifs in other small Tim proteins predicts robust degradation by the protease. Together, these results identify the first specific degron sequence within a native i-AAA protease substrate.

Introduction

Mitochondria are multifunctional organelles that integrate essential activities in eukaryotic cells such as ATP production, calcium signaling, and apoptosis [1,2]. These activities are controlled by a diverse mitochondrial proteome containing ~1200–1500 proteins that are largely encoded in the nucleus [3,4]. Maintaining mitochondrial function therefore requires newly translated polypeptides to be imported from the cytosol and sorted to the correct subcompartment [5–8]. Equally, damaged or unnecessary mitochondrial proteins must be removed by dedicated degradation machinery [9]. Together, these flexible systems of proteostasis must react to the changing energetic demands of the cell and ameliorate the negative consequences of mitochondrial stress [10,11]. Disruption of mitochondrial proteostasis has been implicated in the development of a number of human diseases [1,12,13].

The AAA+ family of proteases plays a major role in monitoring and sculpting the mitochondrial proteome [9]. These ATP-dependent proteases assemble from multiple subunits to form an ATPase ring affixed to a compartmental peptidase chamber [14]. Degradation is accomplished by capturing the energy of successive rounds of ATP binding and hydrolysis to destabilize substrate proteins and translocate the unfolded polypeptides into the peptidase [15–17]. Despite sharing multiple family-specific sequence motifs and similar architectures, different AAA+ proteases recognize and degrade remarkably diverse groups of substrates [18]. Substrate engagement is commonly achieved by the recognition of specific amino acid sequences, known as degrons, which can be located at either substrate termini or internally [18]. Importantly, several individual AAA+ proteases can recognize different classes of degrons that share little sequence homology, indicating versatile modes of substrate recognition within a given protease [18]. This versatility allows diverse proteomes to be regulated by a small number of proteases.

In mitochondria, two hexameric AAA+ proteases (i-AAA and m-AAA) are anchored by transmembrane

Please cite this article as: A. J. Rampello, S. E. Glynn, Identification of a Degradation Signal Sequence within Substrates of the Mitochondrial i-AAA Protease, J. Mol. Biol. (2017), http://dx.doi.org/10.1016/j.jmb.2017.02.009

spans to the inner membrane where they control proteostasis close to the membrane face. Differences in the number of transmembrane spans establish opposing orientations in the inner membrane with the soluble ATPase and protease domains of the i-AAA and m-AAA proteases projecting into the aqueous intermembrane space (IMS) and matrix, respectively [19]. Several degron sequences have been identified for the soluble bacterial AAA+ proteases but no such sequence-specific elements have been identified in known substrates of the mitochondrial AAA proteases [20,21]. Evidence supporting the use of degrons in mitochondrial proteostasis is provided by a number of *in vivo* and *in vitro* studies. For example, the N-terminal presequence of the mitochondrial ribosomal protein MrpL32 is selectively recognized and removed by the m-AAA protease to produce a mature subunit [22]. Additionally, fusion proteins anchored to the inner membrane in yeast were only degraded after temperature-driven unfolding of a domain and the exposure of internal sequences [23]. More recently, solution studies on a rebuilt human i-AAA protease demonstrated the selection of model substrates on the basis of their terminal sequences [24].

Known substrates of the i-AAA protease from *Saccharomyces cerevisiae,* named Yme1p, include the highly homologous small Tim translocase proteins, Tim9 and Tim10 [25,26]. These two soluble IMS proteins assemble into an essential heterohexameric chaperone complex that shuttles newly imported preproteins that are destined for insertion into the inner or outer membrane [27–31]. Crystal structures of the Tim9–Tim10 complex from both yeast and humans display an α-propeller ring of alternating Tim9 and Tim10 subunits [32,33]. Both proteins contain two disulfide bonds encoded by conserved Cys-X_3-Cys motifs. Disruption of these disulfide bonds destabilizes the subunit structure, weakening complex association and accelerating degradation by Yme1p [25]. The observed degradation of these soluble proteins *in vivo* presents them as potential model substrates to study recognition by the i-AAA protease.

Here, we use a rebuilt *S. cerevisiae* Yme1p protease to examine how known mitochondrial substrates are selected for degradation. We show that Tim10 is degraded at a markedly higher rate than Tim9 and that Tim10 degradation is further accelerated by the disruption of its intramolecular disulfide bonds. This substrate preference between the small Tim proteins is conferred by the unstructured N-terminal tentacle of Tim10 that is necessary and sufficient for targeting an unrelated protein for degradation by Yme1p. Major contributions to substrate recognition arise from a phenylalanine-rich motif that predicts the robust degradation of additional members of the small Tim family.

Results

Yme1p degrades Tim10 more rapidly than Tim9

Understanding how Yme1p recognizes specific substrate molecules among the many proteins found in the mitochondrial IMS requires scrutinizing the degradation of biologically relevant substrates. However, *in vitro* studies have been hampered by difficulties in purifying soluble proteases, as individual Yme1p subunits lacking the insoluble transmembrane spans do not assemble into active hexamers [34]. To overcome this, we applied a method used to produce soluble active hexamers of the human YME1L enzyme [24]. A 32-residue hexamerization sequence (cc-hex) [35] was appended to the N terminus of a construct containing the soluble AAA+ and peptidase domains of *S. cerevisiae* Yme1p (residues 267–747) to produce hexYme1p. This enzyme migrated as a hexamer by size-exclusion chromatography, rapidly hydrolyzed ATP (V_{max} = 250 ± 8 min^{-1} enz_6^{-1}; K_M = 116 ± 10 μM), and catalyzed ATP-dependent degradation of the model substrate β-casein (Fig. S1).

We selected the small Tim translocase subunits, Tim9 and Tim10, as candidate proteins to analyze substrate recognition by the protease, as prior *in vivo* studies have indicated that these soluble IMS proteins are degraded by Yme1p [25]. When in complex, each protein adopts a simple helix-loop-helix structure with the two helices cross-linked by dual intramolecular disulfide bonds (Fig. 1a). Tim9 and Tim10 contain extended "tentacles" at the N- and C termini that are predicted to be unstructured and are largely absent in electron density maps, reflecting their disorder in the crystal lattice. We expressed and purified Tim9 and Tim10 fused to a glutathione *S*-transferase (GST) solubility tag that was removed by cleavage with the Tobacco Etch Virus (TEV) protease to leave a three-residue scar (SNA) at the N terminus. The degradation of both proteins by hexYme1p was tested separately in the presence or absence of ATP (Fig. 1b). Both Tim9 and Tim10 were degraded in an ATP-dependent manner, with the loss of Tim10 occurring significantly faster than Tim9. SDS-PAGE band intensities corresponding to the substrates were quantified from multiple experiments, and linear fits to early time points were used to calculate initial rates of degradation (Fig. 1c–d). These measurements showed that Tim10 (0.29 ± 0.04 min^{-1} enz_6^{-1}) is degraded approximately fourfold faster than Tim9 (0.08 ± 0.01 min^{-1} enz_6^{-1}).

Disruption of internal disulfide bonds accelerates Tim10 degradation by Yme1p

Yeast cells containing Tim9 or Tim10 variants bearing substitutions of the disulfide-bond-forming

Please cite this article as: A. J. Rampello, S. E. Glynn, Identification of a Degradation Signal Sequence within Substrates of the Mitochondrial i-AAA Protease, J. Mol. Biol. (2017), http://dx.doi.org/10.1016/j.jmb.2017.02.009

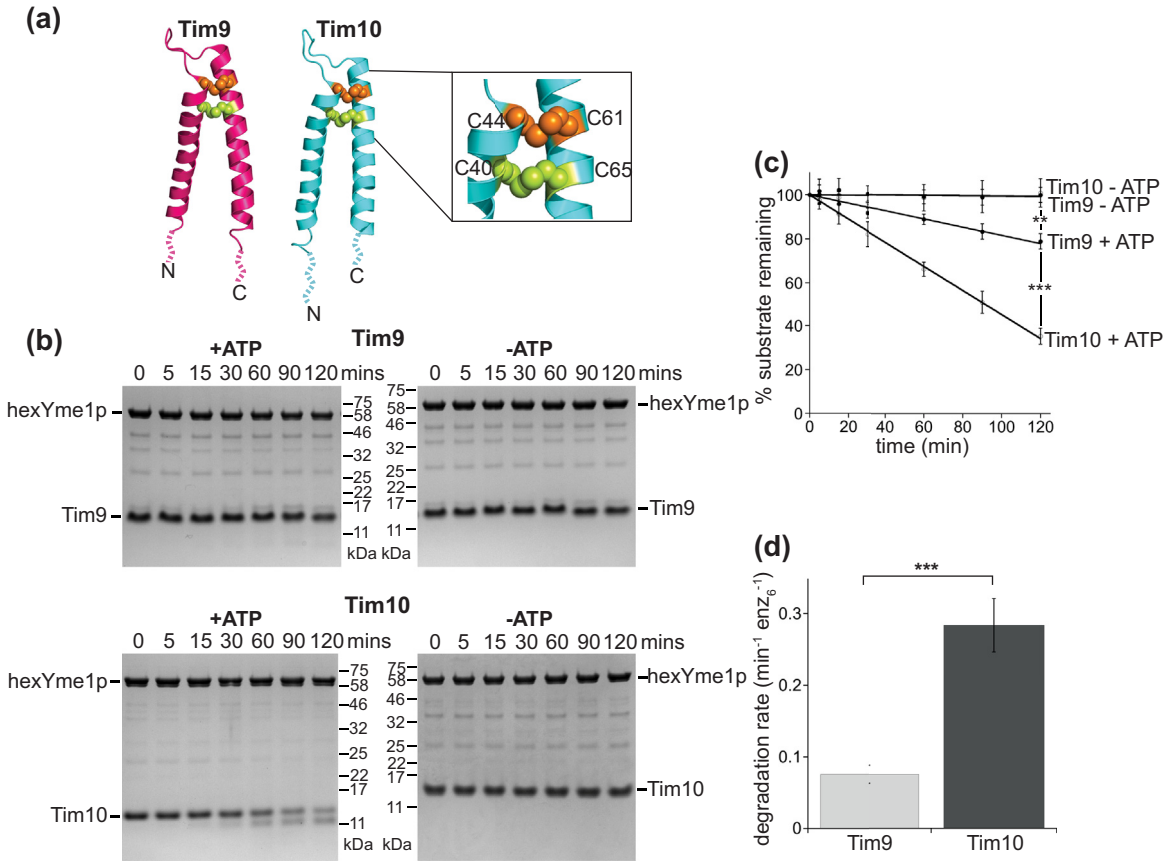

Fig. 1. Degradation of monomeric Tim9 and Tim10 by hexYme1p. (a) Structures of *S. cerevisiae* Tim9 (pink) and Tim10 (cyan) subunits when assembled into the translocase complex (PDB ID: 3DXR). Dotted lines indicate disordered residues at the N- and C termini of both proteins that are missing in the crystal structure. The positions of the outer (lime) and inner (orange) disulfide bonds in both subunits that are shown as spheres and residue numbers for the disulfide bonds in Tim10 are shown (inset). (b) SDS-PAGE images showing the degradation of Tim9 and Tim10 by hexYme1p in the presence or absence of ATP. (c) Plot showing the loss of intensity of SDS-PAGE bands corresponding to substrates from experiments in Fig. 1b. Data points are means of independent replicates ($n = 3$) ± s.d. and lines are linear fits. (d) Initial rates of degradation of Tim9 and Tim10 by hexYme1p calculated from linear fits to early time points from data in Fig. 1c. Values are means of independent replicates ($n = 3$) ± s.d. $^{**}P \leq 0.01$, $^{***}P \leq 0.001$ as calculated using the Student's two-tailed *t*-test.

cysteine residues to serine displayed Yme1p-dependent reduction of both the mutant variants and wild-type counterparts [25]. To investigate the link between cross-linking and proteolysis, we purified Tim9 and Tim10 variants bearing identical substitutions to selectively remove each disulfide bond, and then, we monitored their degradation by hexYme1p (Fig. 2). CD spectroscopy confirmed the loss of helical structure for all variants lacking at least one disulfide bond, comparable to the incubation of the wild-type proteins in 6 M guanidine hydrochloride (Fig. S2). Removal of either the Tim10 "outer" disulfide ($Tim10^{C40S/C65S}$; 0.45 ± 0.01 min^{-1} enz_6^{-1}) or "inner" disulfide ($Tim10^{C44S/C61S}$; 0.42 ± 0.02 min^{-1} enz_6^{-1}) resulted in notably faster degradation rates than wild-type, and removal of both disulfide bonds ($Tim10^{C40S/C44S/C61S/C65S}$; 0.63 ± 0.08 min^{-1} enz_6^{-1}) further increased the rate of degradation (Fig. 2a). Alternatively, disulfide bonds can be removed by chemical reduction to yield free cysteine residues. We incubated wild-type Tim10 with 1 mM DTT at 30 °C for 90 min prior to degradation in the presence of an equal concentration of reducing agent. This reduced protein ($^{DTT}Tim10$) displayed a similar loss of helical structure as the substituted variants (Fig. S2a). Interestingly, $^{DTT}Tim10$ (1.12 ± 0.11 min^{-1} enz_6^{-1}) was degraded at a substantially faster rate than both wild-type Tim10 and the fully substituted variant (Fig. 2a). A similar increase in degradation rate was observed for Tim10 reduced with Tris(2-carboxyethyl)phosphine, yet no increase was observed for the fully substituted variant after DTT treatment

Please cite this article as: A. J. Rampello, S. E. Glynn, Identification of a Degradation Signal Sequence within Substrates of the Mitochondrial i-AAA Protease, J. Mol. Biol. (2017), http://dx.doi.org/10.1016/j.jmb.2017.02.009

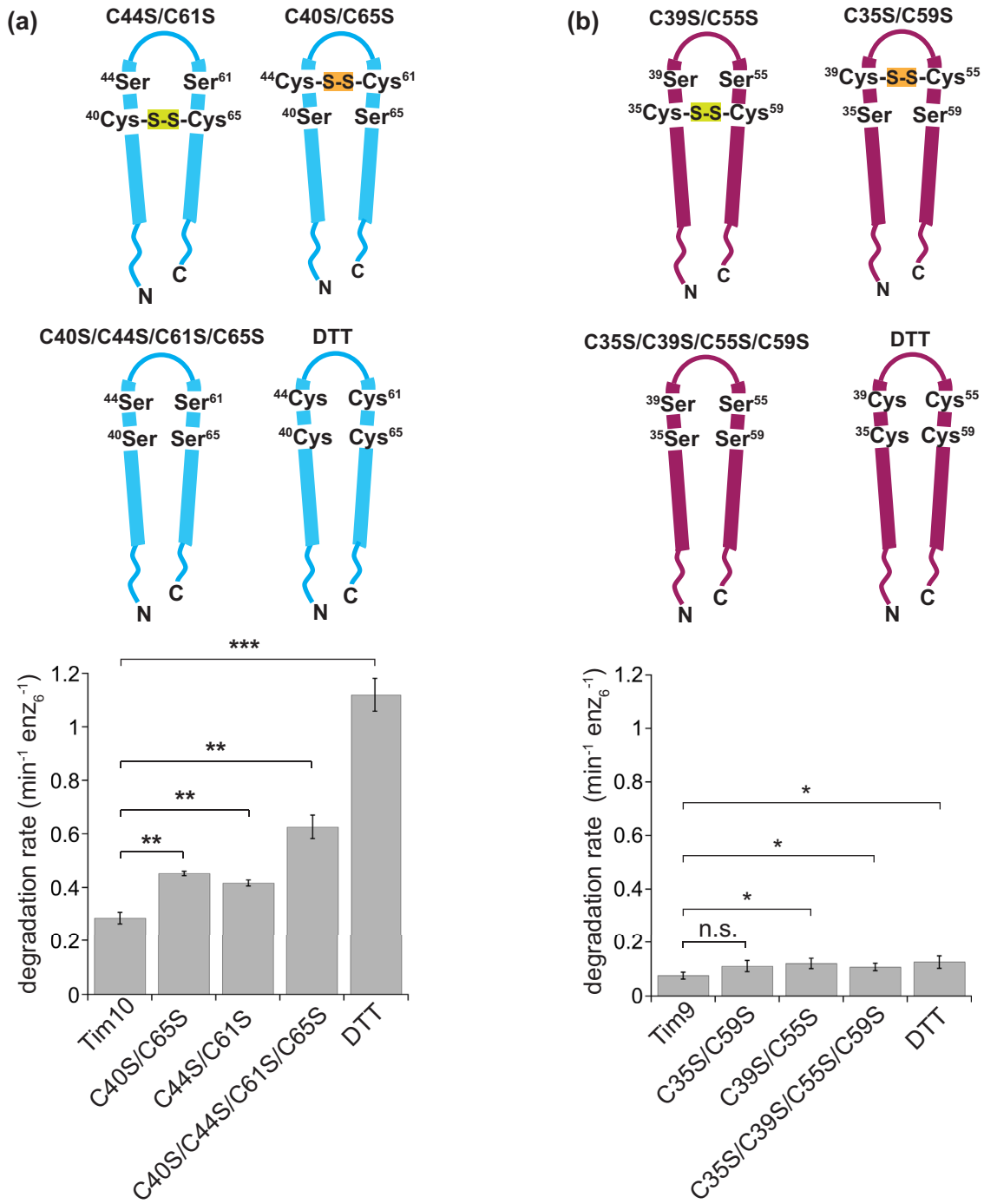

Fig. 2. Disruption of disulfide bonds accelerates Tim10 degradation. (a) Initial degradation rates calculated from SDS-PAGE band intensities are shown for Tim10 variants bearing the substitution to remove the "outer" disulfide bond ($Tim10^{C40S/C65S}$), "inner" disulfide bond ($Tim10^{C44S/C61S}$), or both disulfide bonds ($Tim10^{C40S/C65S/C44S/C61S}$). A chemically reduced species is generated by incubation with DTT ($^{DTT}Tim10$). Removal of either disulfide bond increases the degradation rate with the reduced species displaying the highest rate. (b) Initial degradation rates for variants of Tim9 bearing analogous disruptions of the internal disulfide bonds. No notable change in initial degradation rate is observed after the substitution of the "outer" disulfide bond ($Tim9^{C35S/C59S}$), the "inner" disulfide bond ($Tim9^{C39S/C55S}$), both disulfide bonds ($Tim9^{C35S/C39S/C55S/C59S}$), or after chemical reduction ($^{DTT}Tim9$). Values are means of independent replicates (n = 3) ± s.d. $^{**}P \leq 0.01$, $^{***}P \leq 0.001$ as calculated using the Student's two-tailed t-test.

Please cite this article as: A. J. Rampello, S. E. Glynn, Identification of a Degradation Signal Sequence within Substrates of the Mitochondrial i-AAA Protease, J. Mol. Biol. (2017), http://dx.doi.org/10.1016/j.jmb.2017.02.009

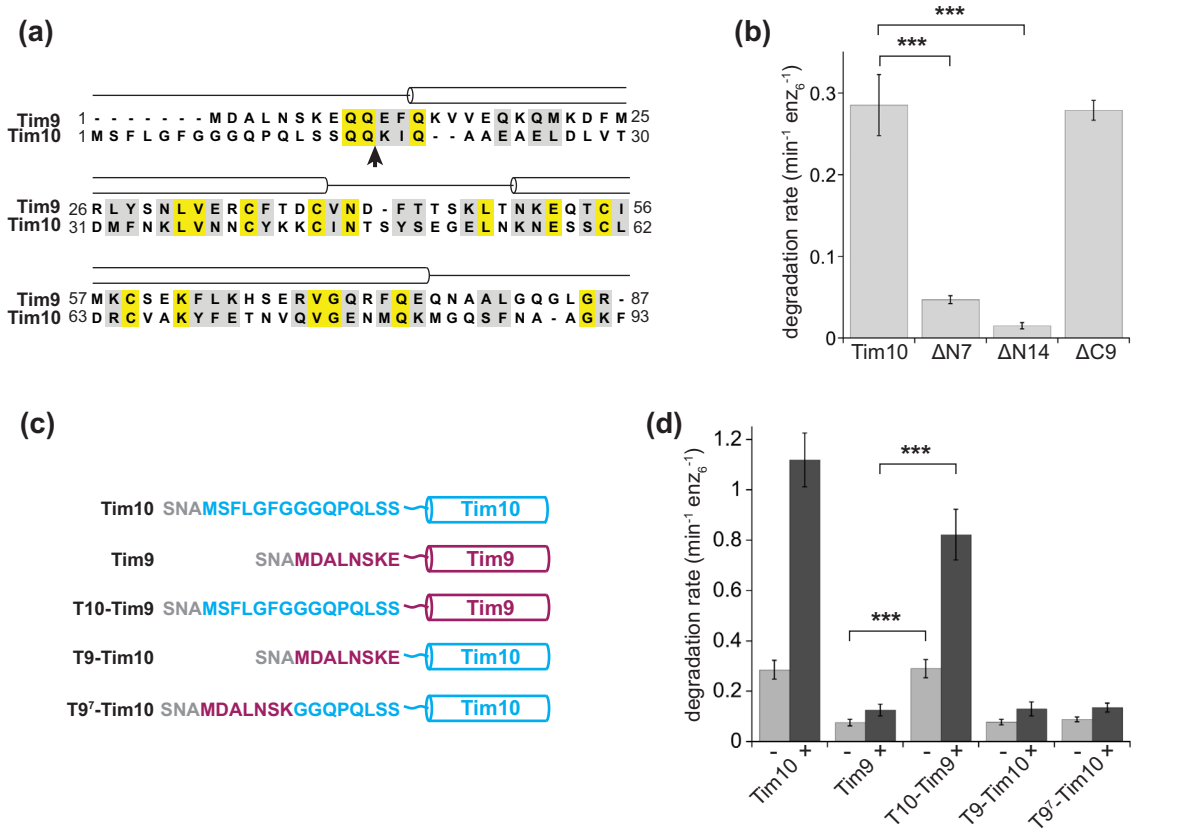

Fig. 3. The N terminus of Tim10 targets the protein for degradation. (a) Structure-based sequence alignment of *S. cerevisiae* Tim9 and Tim10 displaying significant overall sequence homology except at the N-terminal unstructured tentacles. Identical residues (yellow) and conservative substitutions (gray) are highlighted. The N terminus of the partially degraded Tim10 product identified by LC/MS/MS mass spectrometry is indicated with a black arrow. (b) Initial degradation rates calculated from SDS-PAGE band intensities for Tim10 variants bearing truncations of the N- or C termini. Removal of either the N-terminal 7 residues ($Tim10^{\Delta N7}$) or 14 residues ($Tim10^{\Delta N14}$) dramatically reduces the rate of degradation, whereas removal of the C-terminal 9 residues ($Tim10^{\Delta C9}$) has no significant effect. (c) N-terminal sequences of chimeric variants of Tim9 and Tim10 highlighting residues taken from Tim9 (pink) or Tim10 (cyan). Residues colored gray indicate the TEV protease scar. (d) Initial degradation rates of chimeric variants of Tim9 and Tim10. Placing the unstructured N terminus of Tim10 on Tim9 (T10-Tim9) produces rapid degradation, whereas the opposite substitution yields a slowly degraded protein (T9-Tim10). A substrate of equal length as Tim10 but bearing the seven N-terminal residues of Tim9 ($T9^{7}$-Tim10) is slowly degraded. All values are means of independent replicates ($n = 3$) ± s.d. $^{***}P \leq 0.001$ as calculated using the Student's two-tailed *t*-test.

($^{DTT}Tim10^{C40S/C44S/C61S/C65S}$), ruling out a general stimulation of enzyme activity by reducing agent (Fig. S3). Although no large aggregates were observed during purification, we presume that unfolded $Tim10^{C40S/C44S/C61S/C65S}$ can adopt an occluded conformation during expression and purification that is degraded more slowly than the reduced wild-type protein.

In contrast to the effect of disrupting the internal disulfide bonds on the degradation of Tim10, corresponding substitutions in Tim9 produced only small increases in degradation rate in the absence of the "outer" disulfide ($Tim9^{C35S/C59S}$; 0.11 ± 0.02 min^{-1} enz_6^{-1}), "inner" disulfide ($Tim9^{C39S/C55S}$; 0.12 ± 0.02 min^{-1} enz_6^{-1}), or both disulfide bonds ($Tim9^{C35S/C39S/C55S/C59S}$; 0.11 ± 0.02 min^{-1} enz_6^{-1}; Fig. 2b). No significant increase in degradation rate was observed for DTT-treated wild-type Tim9 ($^{DTT}Tim9$; 0.13 ± 0.02 min^{-1} enz_6^{-1}) compared to the fully substituted variant. The experiments described above demonstrate that Tim10 is preferred to Tim9 as a substrate for hexYme1p. If translocation of the disulfide-linked Tim10 polypeptide through the narrow central pore of the protease presents a rate-limiting barrier to degradation, we would expect to observe the increase in rate upon the removal of these bonds. However, the rate-limiting step for a poorly recognized substrate containing similar cross-links, such as Tim9, may be substrate binding and not translocation, and therefore, disruption of the

Please cite this article as: A. J. Rampello, S. E. Glynn, Identification of a Degradation Signal Sequence within Substrates of the Mitochondrial i-AAA Protease, J. Mol. Biol. (2017), http://dx.doi.org/10.1016/j.jmb.2017.02.009

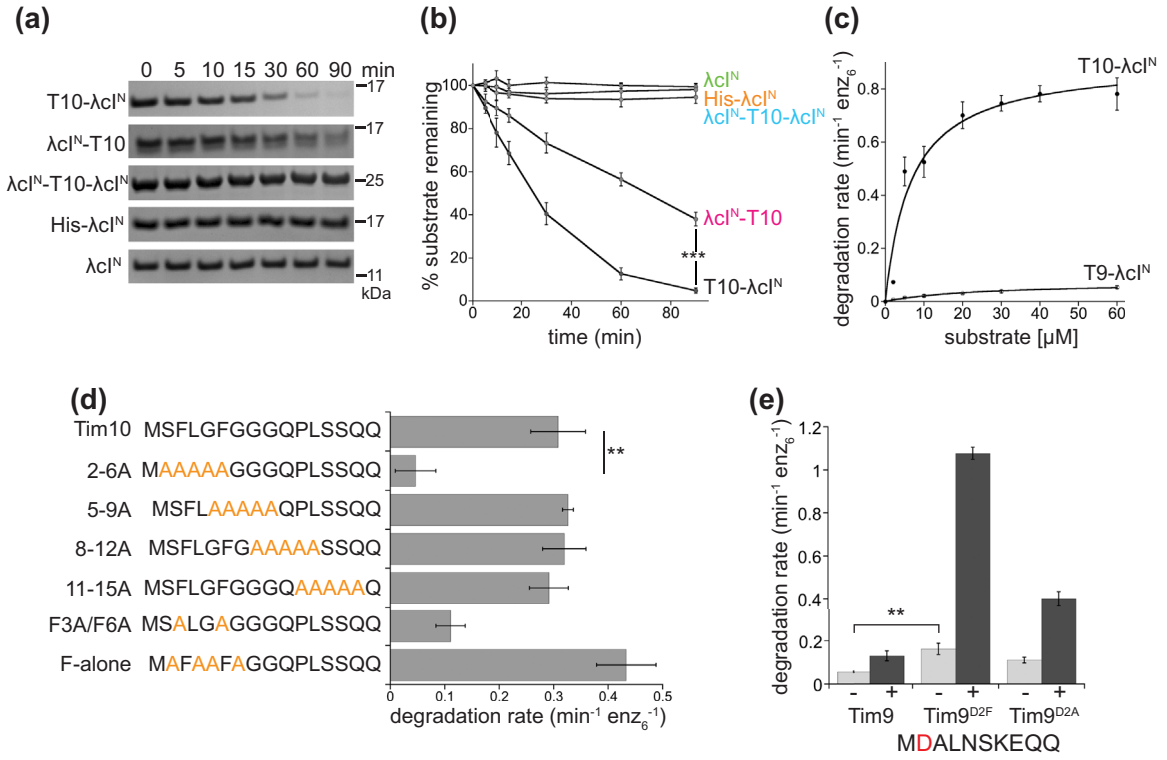

Fig. 4. Identification of a degron sequence within Tim10. (a) SDS-PAGE images showing the degradation of λcl^N constructs containing the T10 sequence at different positions. Rapid degradation is observed when the T10 sequence is positioned at the N terminus (T10-λcl^N) or C terminus (λcl^N–T10), but no significant degradation is observed for the untagged protein (λcl^N), when non-Tim10 residues are placed at the N terminus (His-λcl^N) or when the sequence is placed between two folded copies of λcl^N (λcl^N-T10-λcl^N). (b) Plot showing the quantification of the loss of substrate SDS-PAGE band intensities overtime from the experiments shown in Fig. 4a. (c) Plot showing the degradation rate of T10-λcl^N and T9-λcl^N against initial substrate concentration. Points are averages of independent experiments (n = 3) ± s.d. and are fitted to the Michaelis–Menten equation to calculate the kinetic parameters V_{max} = 0.91 ± 0.07 min^{-1} enz$_6^{-1}$, K_M = 6.7 ± 2.0 μM for T10-λcl^N. In contrast, T9- λcl^N was slowly degraded and could not fully saturate the enzyme. (d) Degradation of Tim10 variants bearing multiple alanine substitutions in the N terminus. N-terminal sequences of each variant are shown with the substituted residues colored orange. Initial degradation rates are shown as horizontal columns. Substitution of residues 5–9 (Tim10$^{5\text{-}9A}$), 8–12 (Tim10$^{8\text{-}12A}$), and 11–15 (Tim10$^{11\text{-}15A}$) had no significant effect on degradation, whereas substitution of residues 2–6 (Tim10$^{2\text{-}6A}$) dramatically reduced the degradation rate. Substitution of Phe3 and Phe6 to alanine (Tim10$^{F3A/F6A}$) also significantly reduced the degradation rate, whereas a substitution of residues 2, 4, 5, and 7 to alanine (Tim10$^{F\text{-}alone}$) was rapidly degraded. (e) Initial degradation rates of Tim9 variants bearing single amino acid substitutions in the N terminus in the absence (–) or presence (+) of DTT. Substitution of Asp2 to phenylalanine (Tim9^{D2F}) induced rapid degradation comparable to Tim10, whereas substitution of this residue to alanine (Tim9^{D2A}) led to a moderate increase. All values are means of independent replicates (n = 3) ± s.d. $^{**}P \leq 0.01$, $^{***}P \leq 0.001$ as calculated using the Student's two-tailed t-test.

disulfide bonds would not be expected to significantly accelerate its degradation.

The N-terminal tentacle of Tim10 targets the protein for degradation by Yme1p

The large difference in degradation rates of Tim9 and Tim10 by hexYme1p is surprising, given the similarity in both sequence and structure. However, a structure-based sequence alignment of Tim9 and Tim10 shows that despite high overall homology, the N-terminal tentacle of Tim10 contains an additional seven residues with significant sequence divergence (Fig. 3a). Given that degron sequences are commonly found at the termini of substrates, we hypothesized that any potential recognition elements for Yme1p are likely to be found in this region.

A series of experiments were used to demonstrate that the N-terminal tentacle of Tim10 is required for the efficient degradation by hexYme1p. Firstly, we purified variants of Tim10 bearing truncations of the unstructured regions at either the N- or C termini. Removal of the N-terminal 7 (Tim10$^{\Delta N7}$) or 14 residues of Tim10 (Tim10$^{\Delta N14}$) resulted in an almost complete loss of degradation by hexYme1p (Fig. 3b). However, a variant lacking nine unstructured

Please cite this article as: A. J. Rampello, S. E. Glynn, Identification of a Degradation Signal Sequence within Substrates of the Mitochondrial i-AAA Protease, J. Mol. Biol. (2017), http://dx.doi.org/10.1016/j.jmb.2017.02.009

residues at the C terminus (Tim10$^{\Delta C9}$) was degraded with a near-identical rate to wild-type Tim10 (0.28 ± 0.01 min^{-1} enz$_6^{-1}$). Degradation of wild-type Tim10 results in the accumulation of a smaller molecular weight product that is only faintly observed during the degradation of Tim10$^{C40S/C44S/C61S/C65S}$ or ^{DTT}Tim10 (Figs. 1b and S5). Matrix-Assisted Laser Desorption/Ionization Time-of-Flight (MALDI-TOF) and Liquid Chromatography Tandem Mass Spectrometry (LC/MS/MS) mass spectrometry identified this product as Tim10 lacking residues 1–16 (Fig. 3a), suggesting that the substrate's N terminus is translocated first into the proteolytic chamber. This partial product only significantly accumulated in variants containing disulfide bonded variants but did not appear to be further degraded. This suggests that stochastic failure to translocate the cross-linked substrate into the proteolytic chamber can lead to the release of a partially degraded product lacking the N terminus, which cannot then be easily reengaged.

We then constructed a number of chimeric substrates with the N-terminal sequences of either Tim9 or Tim10 substituted with those from the partner subunit (Fig. 3c). Replacing the N-terminal 7 residues of Tim9 with the N-terminal 15 residues from Tim10 (T10-Tim9; 0.29 ± 0.04 min^{-1} enz$_6^{-1}$) gave a degradation rate close to wild-type Tim10 that was further increased after reduction by DTT (^{DTT}T10-Tim9; 0.82 ± 0.10 min^{-1} enz$_6^{-1}$; Fig. 3d). However, replacing the N-terminal 15 residues of Tim10 with the N-terminal 7 residues of Tim9 (T9-Tim10; 0.08 ± 0.01 min^{-1} enz$_6^{-1}$) resulted in slow degradation nearly identical to that observed for wild-type Tim9, and DTT treatment produced only a minor increase in degradation rate (^{DTT}T9-Tim10; 0.13 ± 0.03 min^{-1} enz$_6^{-1}$). To ask if the disparity in degradation rate between Tim9 and Tim10 is due to the longer Tim10 N terminus or sequence differences in this region, we replaced only the terminal seven residues of Tim10 with the corresponding seven residues from Tim9, creating a substrate of identical length to Tim10 (T9^7-Tim10). This protein was degraded at a near-identical rate to Tim9 in the absence (0.09 ± 0.01 min^{-1} enz$_6^{-1}$) or presence of DTT (^{DTT}T9^7-Tim10; 0.14 ± 0.01 min^{-1} enz$_6^{-1}$), indicating that the length of the Tim10 N terminus does not drive the faster rate of degradation.

Identification of a degron sequence for Yme1p

The results presented above strongly imply the presence of a degron within the N-terminal tentacle of Tim10. To show that the presence of the TEV protease scar present in substrates expressed as GST fusions does not contribute to degradation, we expressed Tim9, Tim10, and all subsequent substrates using a SUMO/Ulp1 protease system that leaves a native N terminus. No notable difference in degradation rate was seen for either small Tim expressed as a GST or SUMO fusion (Table S1). To demonstrate that the N-terminal tentacle is both necessary and sufficient to direct a protein for degradation by Yme1p, we fused these 15 residues (named T10) to the N terminus of a well-studied protein unrelated to mitochondria, the N-terminal domain of the λcI repressor protein (T10-λcI^N). Rapid degradation was observed for T10-λcI^N but not λcI^N lacking additional residues at the N terminus or a λcI^N variant bearing an N-terminal poly-His tag of similar length to T10 (His-λcI^N ; Fig. 4a–b). The position of the T10 degron on the substrate protein also has a substantial effect on its degradation. Placing the T10 sequence at the C terminus of λcI^N (λcI^N-T10) resulted in significantly slower degradation than T10-λcI^N. However, λcI^N-T10 co-purified with a "clipped" form of the protein that prevented the accurate determination of initial rates (Fig. S8). Insertion of the T10 sequence between two copies of folded λcI^N (λcI^N-T10-λcI^N) produced no measurable degradation that likely reflects a difficulty in engaging the degron at an internal position. Michaelis–Menten kinetic measurements revealed a rapid maximal rate for T10-λcI^N with high affinity (V_{max} = 0.91 ± 0.07 min^{-1} enz$_6^-$; K_M = 6.7 ± 2.0 μM), whereas a construct bearing residues 1–8 of Tim9 at the N terminus (T9-λcI^N) displayed markedly slower degradation and could not saturate the enzyme (Fig. 4c).

To further interrogate the contribution of individual residues in the Tim10 N terminus to recognition by Yme1p, we constructed a series of Tim10 variants bearing substitutions of five consecutive residues to alanine across the length of the unstructured N terminus with a two-residue overlap between each set of substitutions (Fig. 4d). Strikingly, none of these variants displayed diminished degradation rates except for the substitution of residues 2 to 6 (SFLGF; Tim10$^{2\text{-}6A}$), which completely abrogated degradation (0.05 ± 0.04 min^{-1} enz$_6^{-1}$). Our previous study on the degradation of proteins bearing model degron sequences by human hexYME1L identified the sequence FAWFP as a possible recognition motif, and previously identified degrons for the bacterial Lon protease include the sequences WRFAWFP and FGLF [36,37]. These motifs share the consensus sequence F-h-h-F (h = hydrophobic) with the Tim10 N terminus, which suggests that i-AAA proteases may recognize sequences containing phenylalanine residues. Substitution of Phe3 and Phe6 in Tim10 to alanine (Tim10$^{F3A/F6A}$) resulted in a substantial reduction in degradation rate (0.11 ± 0.03 min^{-1} enz$_6^{-1}$), whereas a variant bearing alanine substitutions in all positions immediately surrounding these two phenylalanine residues (Tim10$^{F\text{-}alone}$; ^{1}MAFAAFA^7) was rapidly degraded (0.43 ± 0.06 min^{-1} enz$_6^{-1}$). Furthermore, the introduction of a phenylalanine at position 2 in Tim9

Please cite this article as: A. J. Rampello, S. E. Glynn, Identification of a Degradation Signal Sequence within Substrates of the Mitochondrial i-AAA Protease, J. Mol. Biol. (2017), http://dx.doi.org/10.1016/j.jmb.2017.02.009

($Tim9^{D2F}$; 0.16 ± 0.03 min^{-1} enz_6^{-1}) increased its degradation rate compared to wild-type Tim9 and produced a rate indistinguishable from ^{DTT}Tim10 after the reduction of the disulfide bonds ($^{DTT}Tim9^{D2F}$; 1.07 ± 0.03 min^{-1} enz_6^{-1}; Fig. 4e). As substrate binding to some AAA+ proteases is hindered by the addition of negatively charged residues to the degron, it is possible that the increased degradation rate for $Tim9^{D2F}$ is caused by the removal of the aspartic acid and not the addition of the phenylalanine [20]. An alternative substitution of this residue to alanine ($Tim9^{D2A}$) resulted in a marginal increase in degradation rate of the disulfide-bonded protein (0.11 ± 0.01 min^{-1} enz_6^{-1}) and a moderate increase after treatment with DTT ($^{DTT}Tim9^{D2A}$; 0.40 ± 0.03 min^{-1} enz_6^{-1}) that is significantly lower than $^{DTT}Tim9^{D2F}$. Thus, it appears that while the aspartic acid residue in wild-type Tim9 may provide some barrier to recognition by hexYme1p, the presence of the phenylalanine promotes rapid degradation.

Yme1p recognizes similar sequences in other small Tim proteins

To investigate whether Yme1p uses sequences similar to T10 to recognize other IMS proteins, we examined the degradation of additional members of the small Tim family. In addition to Tim9 and Tim10, yeast contains three other small Tim proteins (Tim8, Tim12, and Tim13) [38]. Tim8 and Tim13 form a complementary chaperone complex Tim9–Tim10 that interacts with an alternative set of substrates [38–41]. Furthermore, a chimeric variant of Tim13 bearing the N terminus of Tim10 can rescue the viability of yeast cells lacking Tim10, suggesting that these subunits play analogous roles in their respective complexes [38]. Tim12 is closely related to Tim10 but remains fixed to the Tim22 complex where it acts as a receptor for proteins shuttled by Tim9–Tim10 [27,38]. Both Tim12 and Tim13 contain conserved phenylalanine residues as part of N-terminal sequences similar to that found in Tim10 (Fig. 5a). We reasoned that hexYme1p should degrade Tim12 and Tim13 more rapidly than Tim8, which does not contain phenylalanine residues in its N terminus. In agreement with this hypothesis, wild-type Tim13 was degraded by hexYme1p at a comparable rate to Tim10 (0.24 ± 0.03 min^{-1} enz_6^{-1}; Fig. 5b–d). However, ^{DTT}Tim13 displayed a more modest increase in degradation rate compared to ^{DTT}Tim10 (0.42 ± 0.10 min^{-1} enz_6^{-1}). Substitution of residues 3–7 in Tim13 (^{3}LSSIF^{7}) to alanine largely eliminated degradation ($Tim13^{3-7A}$; 0.05 ± 0.01 min^{-1} enz_6^{-1}), further strengthening the contribution of phenylalanine residues to recognition by the protease. In contrast, Tim8 was degraded very slowly compared to Tim13 in accordance with its lack of phenylalanine residues (Fig. 5b–c). Full-length

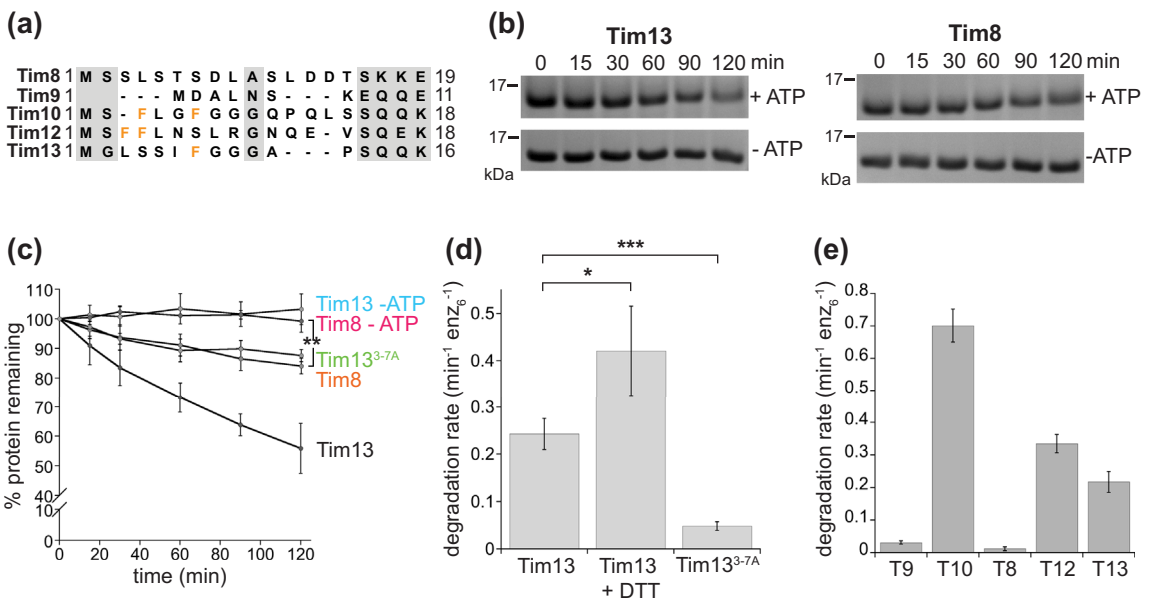

Fig. 5. Additional small Tim proteins are degraded by hexYme1p. (a) Sequence alignment of the N-terminal regions of the small Tim proteins in *S. cerevisiae*. Conservative substitutions are colored gray and phenylalanine residues are highlighted in orange. (b) SDS-PAGE images showing the degradation of Tim13 and of Tim8 in the presence or absence of ATP (c) Quantification of SDS-PAGE substrate band intensities from experiments shown in Fig. 5b. (d) Initial rates of degradation of 20 μM Tim13 in the presence or absence of DTT and $Tim13^{3-7A}$ in the absence of DTT. (e) Initial rates of degradation of 20 μM T8-λcI^{N}, T9-λcI^{N}, T10-λcI^{N}, T12-λcI^{N}, or T13-λcI^{N}. All values are means of independent replicates (n = 3) ± s.d. $^{**}P \leq 0.01$, $^{***}P \leq 0.001$ as calculated using the Student's two-tailed t-test.

Please cite this article as: A. J. Rampello, S. E. Glynn, Identification of a Degradation Signal Sequence within Substrates of the Mitochondrial i-AAA Protease, J. Mol. Biol. (2017), http://dx.doi.org/10.1016/j.jmb.2017.02.009

Tim12 forms high molecular weight aggregates when expressed in isolation and is therefore unsuitable for *in vitro* degradation experiments. To probe the role of the N-terminal regions of these additional small Tim proteins in recognition, we constructed λcI^N variants bearing N-terminal sequences from Tim8 (T8; residues 1–16), Tim12 (T12; 1–15), and Tim13 (T13; 1–13). As predicted, T12-λcI^N (0.33 ± 0.03 min^{-1} enz_6^{-1}) and T13-λcI^N (0.22 ± 0.03 min^{-1} enz_6^{-1}) displayed robust degradation albeit at a slower rate to T10-λcI^N (0.70 ± 0.05 min^{-1} enz_6^{-1}), whereas T8-λcI^N was not degraded at a measurable rate comparable to T9-λcI^N (0.03 ± 0.01 min^{-1} enz_6^{-1}). Taken together, these results strongly suggest that hexYme1p recognizes similar sequences in Tim12 and Tim13 to that present in Tim10.

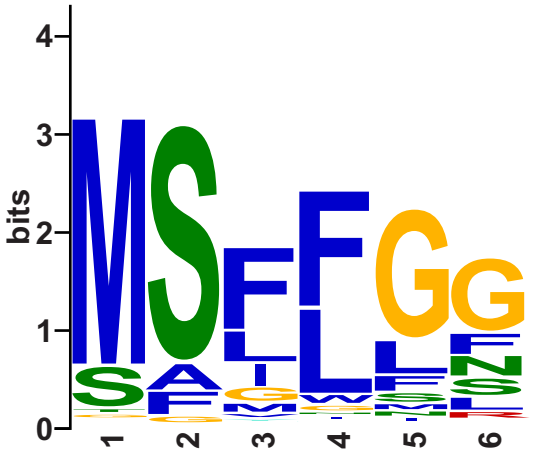

Fig. 6. A conserved N-terminal motif is found across the small Tim family**.** HMM constructed from an alignment of ~300 different Tim10, Tim12, and Tim13 sequences. The HMM was well conserved across these sequences (*E*-value =7.8 e^{-447}).

Discussion

Our results identify a sequence degron within the N-terminal tentacle of Tim10 with key elements located between residue 2 and 6 (SFLGF). Mutational analysis of this region implies an important role for the phenylalanine residues that is strongly supported by the rapid degradation of a Tim9 variant bearing the substitution of a single amino acid to phenylalanine. Furthermore, the presence of similar sequences in the N termini of Tim12 and Tim13 but not Tim8 could predict degradation by the protease. In combination with previous *in vivo* and solution studies on both the yeast and human enzymes, these experiments provide compelling evidence that the i-AAA protease can select substrates for degradation by recognizing specific amino acid sequences. The low complexity of the T10 sequence and subsequent experiments highlighting the importance of phenylalanine residues in recognition may imply that the protease is promiscuous, preferentially engaging nonpolar residues that become exposed after the unfolding of a substrate's hydrophobic core. In this way, the protease could act to remove both specific proteins bearing accessible hydrophobic residues and also damaged or destabilized proteins.

To ask if degron sequences similar to those present in the small Tim proteins are found in other mitochondrial proteins, we curated a library of ~300 Tim10, Tim12, and Tim13 sequences from fungi using NCBI BLAST [42]. This library was used to construct a hidden Markov model (HMM) in MEME [43] containing a consensus N-terminal motif that is well conserved across many of these sequences (*E*-value =2.9 e^{-447}; Fig. 6). This motif is distinct from those discovered surrounding the conserved cysteine residues by a previous analysis that classified the small Tim proteins into four discrete families [38]. The presence of the HMM separates the rapidly degraded small Tim proteins, Tim10 (^{1}MSFLGF^6) and Tim13 (^{3}SSIFGG^8), from the slowly degraded Tim8 and Tim9, which do not contain the sequence. Although we could not purify full-length Tim12 in a suitable form for experiments, based on the rapid degradation of T12-λcI^N and the presence of the N-terminal HMM (^{1}MSFFLN^6), we predict that Tim12 is rapidly degraded by Yme1p in mitochondria. Indeed, levels of Tim12 are significantly enriched in a yeast *yme1* deletion strain compared to wild-type [44].

A search of the *S. cerevisiae* mitochondrial proteome for this HMM identified 68 unique proteins containing motifs with significant similarity ($P \leq 0.0001$) [45]. Of these, 38 are suggested to localize to the IMS, inner, or outer mitochondrial membranes, where they could potentially interact with Yme1p (Table S2). A notable candidate containing the HMM is Tim23 (^{1}MSWLFG^6), the central component of the TIM23 inner membrane translocase complex. This sequence is located within the N-terminal segment that has been proposed to bridge the IMS and insert into the outer membrane during active protein import but may reside in the IMS in the inactive conformation [46,47]. Tim23 has been shown to be degraded in apoptotically stimulated HeLa cells by an undetermined mitochondrial protease that is insensitive to serine protease inhibitors, compatible with the involvement of the i-AAA protease [48].

The experiments described here use a reconstructed *in vitro* system to probe the mechanisms of substrate recognition by Yme1p. Importantly, many of our measurements are consistent with studies examining the loss of small Tim proteins in yeast cells or isolated mitochondria. For example, the observed increase in the degradation rate of Tim10 upon the disruption of the internal disulfide bonds

Please cite this article as: A. J. Rampello, S. E. Glynn, Identification of a Degradation Signal Sequence within Substrates of the Mitochondrial i-AAA Protease, J. Mol. Biol. (2017), http://dx.doi.org/10.1016/j.jmb.2017.02.009

agrees with significantly reduced levels of similarly mutated subunits *in vivo* [25]. The same study indicated that destablilized Tim9 and Tim10 are both degraded by Yme1p, whereas our data clearly show that Tim10 is a superior substrate. While we do observe the slow degradation of Tim9 that may be physiologically relevant, it is possible that the degradation of the small Tim proteins is also influenced by additional factors in the IMS, such as adaptor proteins. Interestingly, pulse-chase experiments revealed that Tim10 is more enriched than Tim9 in a *Δyme1* deletion strain [26]. Moreover, a recent high-resolution mass spectrometry study examining the perturbations of whole proteome levels in single gene knockout strains indicated that the deletion of Yme1p resulted in a greater accumulation of Tim10 than Tim9 [44]. The human Tim10 homolog (TIMM10) contains a shorter unstructured N-terminal tentacle and lacks the consensus motif that we identify in many Tim10 homologs. However, TIMM10 has not been experimentally verified to be a substrate for the human i-AAA protease, YME1L, which is consistent with the differences in sequence at this region. One feature of our experiments is the formation of a partially degraded product that accumulates during the proteolysis of disulfide-bonded Tim10 corresponding to the removal of residues 1–16. It is possible that this species reflects an *in vitro* artifact that is not formed in significant amounts *in vivo*. Moreover, the frequent failure of the protease to translocate cross-linked substrates could indicate that the disruption of the disulfide bonds is needed to stimulate the significant degradation of small Tim proteins in mitochondria. Intriguingly, a product of similar molecular weight can be seen in published pulse-chase experiments that may correspond to the clipped product produced *in vitro* [26].

Assembly of Tim9 and Tim10 into heterohexamers appears to protect the subunits from degradation by Yme1p [25,26]. Two likely scenarios can be envisaged for how the formation of Tim9–Tim10 heterohexamers could impede the degradation of individual Tim10 subunits. As visualized in crystal structures, the complex is stabilized by a number of strong interactions between neighboring subunits, including multiple conserved salt bridges [33]. It is possible that the power stroke of Yme1p is insufficient to overcome these interactions and so prevent the disassembly of the heterohexamer. We have shown previously that the human YME1L protease exhibits a weaker power stroke compared to many other well-studied AAA+ proteases [24]. Alternatively, the formation of the complex may occlude the N terminus of Tim10 and prevent the recognition of the subunit by the protease. Although no such arrangement is seen in the crystal structures of the Tim9–Tim10 complex, the absence of density for these regions prevents us from ruling out this scenario. Further experiments studying mutations in the small Tims that can reduce the stability of the complex will be required to understand how the formation of a complex with Tim9 can protect Tim10 from degradation by Yme1p.

Materials and Methods

Plasmids and proteins

The hexYme1p protease was cloned, expressed, and purified using a similar approach to the previously constructed human hexYME1L protease [24]. A sequence encoding residues 267–747 of *S. cerevisiae* Yme1p was amplified by PCR from genomic DNA and subcloned into a modified 2G-T vector (Addgene #29707) containing a sequence encoding cc-hex (GELKAIAQELKAIAKELKAIAWELKAIAQGAG) immediately C-terminal of the TEV protease cleavage site. The resulting construct contained an N-terminal GST tag followed by the cc-hex sequence and the Yme1p sequence with a 10-residue linker between cc-hex and Yme1p-AP (GSGSYFQSNA; 2G-T-hexYme1p). The hexYme1p^{E381Q} variant was produced by site-directed mutagenesis using the 2G-T-hexYme1p plasmid as a template. All hexYme1p variants were expressed in *Escherichia coli* BL21-CodonPlus cells (Agilent) and purified using an identical protocol to human hexYME1L [24].

Sequences encoding Tim9 and Tim10 were amplified by PCR from *S. cerevisiae* genomic DNA and subcloned into either the 2G-T vector (2G-T-Tim9, 2G-T-Tim10) or the pET His_6 SUMO vector (2S-T; Addgene #29711) that was modified to remove the TEV protease cleavage site (2S-U; 2-S-U-Tim9, 2S-U-Tim10). All cysteine-to-serine substitutions and chimeric variants of Tim9 and Tim10 were introduced by site-directed mutagenesis using the 2G-T-Tim9 and 2G-T-Tim10 plasmids as templates. All other variants of Tim9 and Tim10 were produced by site-directed mutagenesis using the 2S-U-Tim9 and 2S-U-Tim10 plasmids as templates. Sequences encoding Tim8 and Tim13 were amplified by PCR from *S. cerevisiae* genomic DNA and subcloned into the 2S-U vector. Alanine subsitutions were introduced by site-directed mutagenesis using the 2-S-U-Tim13 plasmid as a template. All small Tim variants were grown in *E. coli* Origami (DE3) (pLysS; Novagen) at 37 °C in LB supplemented with ampicillin (100 μg/mL) and chloramphenicol (34 μg/mL). Protein expression was induced by the addition of 1 mM IPTG at an OD_{600} of 0.6–0.8 and grown for 16 h at 16 °C. Cells expressing GST-fusion variants were harvested by centrifugation, resuspended in GST lysis buffer [20 mM Tris–HCl (pH 8.0), 150 mM NaCl, 5% glycerol, and 1 mM PMSF], and lysed by

Please cite this article as: A. J. Rampello, S. E. Glynn, Identification of a Degradation Signal Sequence within Substrates of the Mitochondrial i-AAA Protease, J. Mol. Biol. (2017), http://dx.doi.org/10.1016/j.jmb.2017.02.009

sonication. Lysates were clarified by centrifugation at 15,000 rpm for 30 min and purified by GST affinity chromatography using an identical protocol to hexYme1p. Cells expressing SUMO fusions were resuspended in SUMO lysis buffer [20 mM Tris–HCl (pH 8.0), 400 mM NaCl, 100 mM KCl, 5% glycerol, and 10 mM imidazole] supplemented with 1 mM PMSF and lysed by sonication. Lysate was clarified by centrifugation, and the supernatant was loaded onto a Ni-NTA agarose resin (Thermo Scientific) gravity column. Resin was washed with SUMO lysis buffer supplemented with 50 mM imidazole and eluted with SUMO elution buffer [20 mM Tris–HCl (pH 8.0), 400 mM NaCl, 100 mM KCl, 5% glycerol, and 250 mM imidazole]. His_6Ulp1 protease (~0.2 mg/mL) was added to the eluted proteins and incubated for 16 h at 4 °C followed by buffer exchange using a HiTrap Desalting column (GE Healthcare) into PD buffer. His_6SUMO and His_6Ulp1 were removed by the addition of the protein suspension over a Ni-NTA agarose (Thermo Scientific) gravity column. Size-exclusion chromatography for all small Tim variants was carried out using a Superdex-75 10/300 GL column (GE Healthcare) pre-equilibrated with PD buffer [25 mM Hepes (pH 8.0), 100 mM KCl, 5% glycerol, and 5 mM $MgCl_2$].

A plasmid containing the sequence of λcI^N was a gift from Dr. Robert Sauer (MIT). The sequence encoding λcI^N was subcloned into the 2S-U vector (2S-U-λcI^N), and all variants of λcI^N were constructed by site-directed mutagenesis using the 2S-U-λcI^N plasmid as a template. All 2S-U-λcI^N variants were expressed in the *E. coli* strain BL21 (DE3). Expression and purification of all variants followed an identical procedure to the 2S-U-Tim proteins.

Analytical size-exclusion chromatography

Analytical size-exclusion chromatography experiments were carried out by injecting ~1 mg of protein in a volume of 200 µl onto a Superose 6 Increase 10/300 GL column (GE Healthcare). Apparent molecular weights were calculated from a standard curve determined from the elution of molecular weight standards (Biorad).

CD spectroscopy

CD spectra were collected using an Applied Photophysics Chirascan spectrometer with a 1-mm path length quartz cuvette. Prior to data collection, all proteins were buffer exchanged into 5 mM Tris–HCl (pH 8.0) using Micro Bio-Spin 6 columns (Bio Rad). Spectra shown are the average of three scans from 190 to 260 nm (0.5-s averaging time) with a 0.2-nm step size at 30 °C. DTT-treated samples were incubated in 1 mM DTT at 30 °C for 1.5 h prior to data acquisition. Spectra collected on buffer without protein were subtracted from each spectrum.

Biochemical assays

ATPase assays were conducted as described previously [49]. All reactions contained 0.2 µM hexYme1 in PD buffer at 30 °C. Reactions were carried out in a 384-well clear bottom plate (Corning) using a SpectraMax M5 plate reader (Molecular Devices). Protein degradation reactions were performed at 30 °C in 75 µL or 90 µL total volume containing 0.5 µM enzyme in PD buffer and an ATP regeneration system when appropriate (5 mM ATP, 20 mM phosphoenolpyruvate, and 18.75 U ml^{-1} pyruvate kinase). Then, 12 µL aliquots were removed at appropriate time and quenched in Laemli loading buffer containing 2% SDS at 90 °C for 5 min. Chemical reduction of Tim proteins was performed by incubating proteins in the presence of 1 mM DTT or Tris(2-carboxyethyl)phosphine at 30 °C for 90 min prior to the initiation of degradation reactions supplemented with an equal concentration of reducing agent. Substrate degradation was visualized on 12% SDS-PAGE stained with Coomassie Blue R-250. Loss of full-length substrate band intensities was quantified using ImageJ [50], and initial degradation rates were calculated from at least five time points in the linear range. All intensities were normalized to 100% full-length substrate at 0 s [51]. Representative uncropped SDS-PAGE images for all degradation experiments are shown in the Supplementary Figures. All calculated initial degradation rates are shown in Table S1.

Mass spectrometry

MALDI-TOF was carried out using a Voyager-DE STR (Applied Biosystems) on trypsin-digested SDS-PAGE gel slices containing either full-length wild-type Tim10 or the smaller molecular weight product. A peptide corresponding to residues 1–18 was missing in the smaller product. LC/MS/MS was carried out on identical samples using a Thermo LTQ Orbitrap XL Ion Trap Mass Spectrometer (Thermo Fisher) in Information Dependent Analysis, positive ion mode. Sequence coverage was found for all residues in the wild-type control and missing residues 1 to 16 in the smaller product.

Acknowledgments

We thank the Stony Brook Proteomics Center for help with mass spectrometry. We thank Dan Raleigh, Steve Smith, and Wali Karzai for providing access to instrumentation. We thank Robert Sauer for supplying the plasmid encoding the λcI^N protein. We thank Chris Giuliano, Hui Shi, and Bojian Ding for helpful discussions. The Stony Brook Proteomics Center was supported by the shared instrumentation grant NIH/NCRR 1 S10 RR023680-1. A.J.R was

Please cite this article as: A. J. Rampello, S. E. Glynn, Identification of a Degradation Signal Sequence within Substrates of the Mitochondrial i-AAA Protease, J. Mol. Biol. (2017), http://dx.doi.org/10.1016/j.jmb.2017.02.009

supported by National Institutes of Health training grant T32 GM008468. This work was supported by National Institutes of Health grant R01 GM115898.

Author contributions: A.J.R conducted all experiments. A.J.R. and S.E.G. contributed to experimental design, data interpretation, and writing of the manuscript.

Conflict of interest: The authors declare no competing financial interest.

Appendix A. Supplementary Data

Supplementary data to this article can be found online at http://dx.doi.org/10.1016/j.jmb.2017.02.009.

Received 12 December 2016;
Received in revised form 10 February 2017;
Accepted 11 February 2017
Available online xxxx

Keywords:
mitochondria;
protein quality control;
AAA+;
degron;
intermembrane space

Abbreviations used:
IMS, intermembrane space; GST, glutathione *S*-transferase; HMM, hidden Markov model; MALDI-TOF, Matrix-Assisted Laser Desorption/Ionization Time-of-Flight; LC/MS/MS, Liquid Chromatography Tandem Mass Spectrometry; TEV, Tobacco Etch Virus.

References

[1] D.C. Chan, Mitochondria: dynamic organelles in disease, aging, and development, Cell 125 (2006) 1241–1252.
[2] H.M. McBride, M. Neuspiel, S. Wasiak, Mitochondria: more than just a powerhouse, Curr. Biol. 16 (2006) R551–R560.
[3] M.F. Lopez, B.S. Kristal, E. Chernokalskaya, A. Lazarev, A.I. Shestopalov, A. Bogdanova, et al., High-throughput profiling of the mitochondrial proteome using affinity fractionation and automation, Electrophoresis 21 (2000) 3427–3440.
[4] S.E. Calvo, K.R. Clauser, V.K. Mootha, MitoCarta2.0: an updated inventory of mammalian mitochondrial proteins, Nucleic Acids Res. 44 (2016) D1251–D1257.
[5] N. Pfanner, A. Geissler, Versatility of the mitochondrial protein import machinery, Nat. Rev. Mol. Cell Biol. 2 (2001) 339–349.
[6] C.M. Koehler, New developments in mitochondrial assembly, Annu. Rev. Cell Dev. Biol. 20 (2004) 309–335.
[7] M.J. Baker, A.E. Frazier, J.M. Gulbis, M.T. Ryan, Mitochondrial protein-import machinery: correlating structure with function, Trends Cell Biol. 17 (2007) 456–464.
[8] W. Neupert, J.M. Herrmann, Translocation of proteins into mitochondria, Annu. Rev. Biochem. 76 (2007) 723–749.
[9] T. Tatsuta, T. Langer, AAA proteases in mitochondria: diverse functions of membrane-bound proteolytic machines, Res. Microbiol. 160 (2009) 711–717.
[10] T.K. Rainbolt, N. Atanassova, J.C. Genereux, R.L. Wiseman, Stress-regulated translational attenuation adapts mitochondrial protein import through Tim17A degradation, Cell Metab. 18 (2013) 908–919.
[11] T.K. Rainbolt, J. Lebeau, C. Puchades, R.L. Wiseman, Reciprocal degradation of YME1L and OMA1 adapts mitochondrial proteolytic activity during stress, Cell Rep. 14 (2016) 2041–2049.
[12] J.Q. Kwong, M.F. Beal, G. Manfredi, The role of mitochondria in inherited neurodegenerative diseases, J. Neurochem. 97 (2006) 1659–1675.
[13] M.T. Lin, M.F. Beal, Mitochondrial dysfunction and oxidative stress in neurodegenerative diseases, Nature 443 (2006) 787–795.
[14] R.T. Sauer, T.A. Baker, AAA+ proteases: ATP-fueled machines of protein destruction, Annu. Rev. Biochem. 80 (2011) 587–612.
[15] A. Martin, T.A. Baker, R.T. Sauer, Rebuilt AAA + motors reveal operating principles for ATP-fuelled machines, Nature 437 (2005) 1115–1120.
[16] S.E. Glynn, A. Martin, A.R. Nager, T.A. Baker, R.T. Sauer, Structures of asymmetric ClpX hexamers reveal nucleotide-dependent motions in a AAA+ protein-unfolding machine, Cell 139 (2009) 744–756.
[17] B.M. Stinson, A.R. Nager, S.E. Glynn, K.R. Schmitz, T.A. Baker, R.T. Sauer, Nucleotide binding and conformational switching in the hexameric ring of a AAA+ machine, Cell 153 (2013) 628–639.
[18] T.A. Baker, R.T. Sauer, ATP-dependent proteases of bacteria: recognition logic and operating principles, Trends Biochem. Sci. 31 (2006) 647–653.
[19] K. Leonhard, J.M. Herrmann, R.A. Stuart, G. Mannhaupt, W. Neupert, T. Langer, AAA proteases with catalytic sites on opposite membrane surfaces comprise a proteolytic system for the ATP-dependent degradation of inner membrane proteins in mitochondria, EMBO J. 15 (1996) 4218–4229.
[20] J.M. Flynn, I. Levchenko, M. Seidel, S.H. Wickner, R.T. Sauer, T.A. Baker, Overlapping recognition determinants within the ssrA degradation tag allow modulation of proteolysis, Proc. Natl. Acad. Sci. U. S. A. 98 (2001) 10,584–10,589.
[21] E. Gur, R.T. Sauer, Degrons in protein substrates program the speed and operating efficiency of the AAA+ Lon proteolytic machine, Proc. Natl. Acad. Sci. U. S. A. 106 (2009) 18,503–18,508.
[22] F. Bonn, T. Tatsuta, C. Petrungaro, J. Riemer, T. Langer, Presequence-dependent folding ensures MrpL32 processing by the m-AAA protease in mitochondria, EMBO J. 30 (2011) 2545–2556.
[23] K. Leonhard, B. Guiard, G. Pellecchia, A. Tzagoloff, W. Neupert, T. Langer, Membrane protein degradation by AAA proteases in mitochondria: extraction of substrates from either membrane surface, Mol. Cell 5 (2000) 629–638.
[24] H. Shi, A.J. Rampello, S.E. Glynn, Engineered AAA+ proteases reveal principles of proteolysis at the mitochondrial inner membrane, Nat. Commun. 7 (2016) 13,301.
[25] M.J. Baker, V.P. Mooga, B. Guiard, T. Langer, M.T. Ryan, D. Stojanovski, Impaired folding of the mitochondrial small TIM chaperones induces clearance by the i-AAA protease, J. Mol. Biol. 424 (2012) 227–239.

[26] M.P. Spiller, L. Guo, Q. Wang, P. Tran, H. Lu, Mitochondrial Tim9 protects Tim10 from degradation by the protease Yme1, Biosci. Rep. 35 (2015), http://dx.doi.org/10.1042/BSR20150038.
[27] C.M. Koehler, E. Jarosch, K. Tokatlidis, K. Schmid, R.J. Schweyen, G. Schatz, Import of mitochondrial carriers mediated by essential proteins of the intermembrane space, Science 279 (1998) 369–373.
[28] C.M. Koehler, The small Tim proteins and the twin Cx3C motif, Trends Biochem. Sci. 29 (2004) 1–4.
[29] N. Wiedemann, A.E. Frazier, N. Pfanner, The protein import machinery of mitochondria, J. Biol. Chem. 279 (2004) 14,473–14,476.
[30] N. Bolender, A. Sickmann, R. Wagner, C. Meisinger, N. Pfanner, Multiple pathways for sorting mitochondrial precursor proteins, EMBO Rep. 9 (2008) 42–49.
[31] E. Ceh-Pavia, M.P. Spiller, H. Lu, Folding and biogenesis of mitochondrial small Tim proteins, Int. J. Mol. Sci. 14 (2013) 16,685–16,705.
[32] C.T. Webb, M.A. Gorman, M. Lazarou, M.T. Ryan, J.M. Gulbis, Crystal structure of the mitochondrial chaperone TIM9.10 reveals a six-bladed alpha-propeller, Mol. Cell 21 (2006) 123–133.
[33] M.J. Baker, C.T. Webb, D.A. Stroud, C.S. Palmer, A.E. Frazier, B. Guiard, et al., Structural and functional requirements for activity of the Tim9–Tim10 complex in mitochondrial protein import, Mol. Biol. Cell 20 (2009) 769–779.
[34] K. Leonhard, A. Stiegler, W. Neupert, T. Langer, Chaperone-like activity of the AAA domain of the yeast Yme1 AAA protease, Nature 398 (1999) 348–351.
[35] N.R. Zaccai, B. Chi, A.R. Thomson, A.L. Boyle, G.J. Bartlett, M. Bruning, et al., A de novo peptide hexamer with a mutable channel, Nat. Chem. Biol. 7 (2011) 935–941.
[36] E. Gur, R.T. Sauer, Recognition of misfolded proteins by Lon, a AAA(+) protease, Genes Dev. 22 (2008) 2267–2277.
[37] M. Gonzalez, E.G. Frank, A.S. Levine, R. Woodgate, Lon-mediated proteolysis of the *Escherichia coli* UmuD mutagenesis protein: *in vitro* degradation and identification of residues required for proteolysis, Genes Dev. 12 (1998) 3889–3899.
[38] I.E. Gentle, A.J. Perry, F.H. Alcock, V.A. Likic, P. Dolezal, E.T. Ng, et al., Conserved motifs reveal details of ancestry and structure in the small TIM chaperones of the mitochondrial intermembrane space, Mol. Biol. Evol. 24 (2007) 1149–1160.
[39] D. Leuenberger, N.A. Bally, G. Schatz, C.M. Koehler, Different import pathways through the mitochondrial intermembrane space for inner membrane proteins, EMBO J. 18 (1999) 4816–4822.
[40] A.J. Davis, N.N. Alder, R.E. Jensen, A.E. Johnson, The Tim9p/10p and Tim8p/13p complexes bind to specific sites on Tim23p during mitochondrial protein import, Mol. Biol. Cell 18 (2007) 475–486.
[41] K.N. Beverly, M.R. Sawaya, E. Schmid, C.M. Koehler, The Tim8-Tim13 complex has multiple substrate binding sites and binds cooperatively to Tim23, J. Mol. Biol. 382 (2008) 1144–1156.
[42] N.R. Coordinators, Database resources of the National Center for biotechnology information, Nucleic Acids Res. 44 (2016) D7–19.
[43] T.L. Bailey, M. Boden, F.A. Buske, M. Frith, C.E. Grant, L. Clementi, et al., MEME SUITE: tools for motif discovery and searching, Nucleic Acids Res. 37 (2009) W202–W208.
[44] B.J. Floyd, E.M. Wilkerson, M.T. Veling, C.E. Minogue, C. Xia, E.T. Beebe, et al., Mitochondrial protein interaction mapping identifies regulators of respiratory chain function, Mol. Cell 63 (2016) 621–632.
[45] A. Sickmann, J. Reinders, Y. Wagner, C. Joppich, R. Zahedi, H.E. Meyer, et al., The proteome of *Saccharomyces cerevisiae* mitochondria, Proc. Natl. Acad. Sci. U. S. A. 100 (2003) 13,207–13,212.
[46] M. Donzeau, K. Kaldi, A. Adam, S. Paschen, G. Wanner, B. Guiard, et al., Tim23 links the inner and outer mitochondrial membranes, Cell 101 (2000) 401–412.
[47] D. Popov-Celeketic, K. Mapa, W. Neupert, D. Mokranjac, Active remodelling of the TIM23 complex during translocation of preproteins into mitochondria, EMBO J. 27 (2008) 1469–1480.
[48] C.G. Goemans, P. Boya, C.J. Skirrow, A.M. Tolkovsky, Intramitochondrial degradation of Tim23 curtails the survival of cells rescued from apoptosis by caspase inhibitors, Cell Death Differ. 15 (2008) 545–554.
[49] J.G. Norby, Coupled assay of Na+,K+-ATPase activity, Methods Enzymol. 156 (1988) 116–119.
[50] C.A. Schneider, W.S. Rasband, K.W. Eliceiri, NIH image to ImageJ: 25 years of image analysis, Nat. Methods 9 (2012) 671–675.
[51] E. Gur, M. Vishkautzan, R.T. Sauer, Protein unfolding and degradation by the AAA+ Lon protease, Protein Sci. 21 (2012) 268–278.

Please cite this article as: A. J. Rampello, S. E. Glynn, Identification of a Degradation Signal Sequence within Substrates of the Mitochondrial i-AAA Protease, J. Mol. Biol. (2017), http://dx.doi.org/10.1016/j.jmb.2017.02.009